



Published in final edited form as:

IEEE Antennas Propag Mag. 2015 February ; 174(1): 164–176. doi:10.1109/MAP.2015.2397157.

A Hybrid Approach for Efficient Modeling of Medium-Frequency Propagation in Coal Mines

Donovan E. Brocker¹, Peter E. Sieber¹, Joseph A. Waynert², Jingcheng Li², Pingjuan L. Werner¹, and Douglas H. Werner¹

Joseph A. Waynert: JWaynert@CDC.gov; Jingcheng Li: JLi6@CDC.gov; Douglas H. Werner: dhw@psu.edu

¹Pennsylvania State University, University Park, PA 16802 USA

²National Institute for Occupational Safety and Health, Pittsburgh, PA 15236 USA

Abstract

An efficient procedure for modeling medium frequency (MF) communications in coal mines is introduced. In particular, a hybrid approach is formulated and demonstrated utilizing ideal transmission line equations to model MF propagation in combination with full-wave sections used for accurate simulation of local antenna-line coupling and other near-field effects. This work confirms that the hybrid method accurately models signal propagation from a source to a load for various system geometries and material compositions, while significantly reducing computation time. With such dramatic improvement to solution times, it becomes feasible to perform large-scale optimizations with the primary motivation of improving communications in coal mines both for daily operations and emergency response. Furthermore, it is demonstrated that the hybrid approach is suitable for modeling and optimizing large communication networks in coal mines that may otherwise be intractable to simulate using traditional full-wave techniques such as moment methods or finite-element analysis.

Keywords

Coal mines; communication network optimization; medium frequency (MF); propagation; transmission lines (TLs)

1. Introduction

Throughout history, mining tragedies have emphasized the need for communication systems in the mining industry with improved survivability. In response to such types of disasters, the United States Congress passed the Mine Improvement and New Emergency Response Act (MINER Act) in 2006, considered to be the most significant mine safety legislation since the Federal Mine Safety and Health Act of 1977. Over the years, researchers have performed extensive research on the design optimization and implementation of communication systems for use in coal mining operations [1–5]. A large range of frequencies have been proposed for various types of coal mine communications, ranging from very-high-frequency and ultrahigh-frequency technologies [6–15], typically for in-mine daily operations, to emergency tracking systems [16–20] based on very-low-frequency through-the-earth technologies. MFs have also been proposed for in-mine communications [8], [21–30], which is the focus of this paper.

MFs are identified for their ability to parasitically couple into conductor infrastructure within a mine tunnel and propagate large distances through various room-and-pillar architectures with relatively low attenuation [27, 28]. In practice, this means that a medium frequency (MF) system may take advantage of existing conductor infrastructure in a coal mine, only requiring wireless handhelds for communications. Examples of typical conductors in mines include trolley rails, lighting and telephone wiring, and machinery power cables. Another advantage of MF signals is their ability to propagate hundreds of meters through the coal seam without man-made metal conductors present [31, 32], because the relative conductivities of the coal and surrounding rock layers can form a suitable waveguide. As mandated by the MINER Act, current research efforts are to primarily focus on improving the survivability of existing technologies and developing new solutions for emergency tracking. Hence, the characteristics outlined above make MF communications attractive for day-to-day mining operations as well as in the event of an emergency, although the low carrier frequency generally limits the system to a single channel. As a result, there is a renewed interest in MF technologies [33–38] to address this mandate.

The current modes that can be excited along multiple-conductor configurations within a coal mine tunnel are characterized as differential mode (DM) and common mode (CM) propagations. DM refers to propagation 180 degrees out of phase along conductors; CM refers to in-phase propagation along conductor networks whereby currents return through surrounding mine-earth boundaries. Many times, one mode is dominant in a communication system; however, the most general propagation is a superposition of both CM and DM. Furthermore, CM and DM propagation modes can experience discernible differences in attenuation and coupling efficiency from antenna to transmission line (TL) [39–41]. Because of these differences, accurate modeling of both modes is crucial for understanding and optimizing MF communications in coal mines. The remainder of this paper will demonstrate the proposed hybrid approach by concentrating on each mode individually and leaves multimodal (or multiconductor) TL analysis for consideration in future work. Looking forward, when the proposed hybrid approach is extended to accommodate multiconductor systems, it will be constructed in the same way as outlined in this paper, with the difference in that TL models would be represented by matrix equations to accommodate multiconductor configurations [42–44].

In order to determine what factors most influence the behavior of MF propagation in coal mines, extensive numerical and analytical modeling is required. Many previous models of MF propagation in earth-bounded systems [45, 46] develop modal equations that require sophisticated numerical methods in order to facilitate accurate calculations. Alternatively, constructing representative models using commercial method of moments (MoM) codes presents a separate challenge because they require considerable computational resources and time. For example, a typical coal mine tunnel cross section is on the order of meters, suggesting information about the meshing resolution of the MoM model; meanwhile, the length of a mine may be on the order of kilometers, indicating the overall size of the model. Hence, full-wave simulation of signal propagation from one end of a mine to another can become an extremely large problem for traditional computational electromagnetic (EM) modeling codes. The hybrid approach outlined and demonstrated in the following sections mitigates this challenge. The general concept is illustrated in Figure 1, showing “black box”

regions of interest that are to be modeled using MoM. These sections could contain a source/transmitter coupling to a TL, a load/receiver receiving a signal from a TL, or a line break and scattered overburden due to a mine collapse; essentially, these sections are used to model anything not trivially represented by simple analytical expressions. In contrast, the interconnects for these regions are typically a network of conductors, or a TL, providing a uniform path for MF propagation and hence can be modeled with simple TL equations. This technique allows for efficient simulation of communication paths while providing modeling flexibility and enabling parametric investigations of the source and receiver/load sections in addition to effects associated with mining disaster events. Exhaustive parametric studies of excitation (i.e., antenna-line coupling) and line termination types would be impractical, if not impossible, if the entire propagation path in a given communication link were modeled using full-wave techniques alone. As will be demonstrated, this hybrid approach significantly reduces the amount of computational resources and time required to make calculations of interest.

Ultimately, a primary objective of this work is to facilitate system-level optimization of coal mine communication networks. For example, optimizations may include maximizing power transfer from a transmitting antenna to a receiving antenna and minimizing standing-wave ratio (SWR). Another goal may be to design an MF communication system that is more survivable during disaster events. In order to efficiently optimize such large problems, specialized global search algorithms were used in conjunction with the proposed hybrid model to analyze fitness of candidate network designs. Such an optimization technique, which may require hundreds or even thousands of function evaluations, would not be feasible without the significant improvement of solution times afforded by the hybrid approach. For demonstration, the final example in this work minimized SWR near the transmitting and receiving antennas of an MF communication network. Subsequently, a line break was introduced to the previously optimized design, simulating the event of a mine collapse. Once again, the hybrid approach was applied by modeling the broken TL with a full-wave region, and it was shown to accurately reproduce the corresponding propagation effects and power losses. These effects would be difficult to reproduce applying only TL equations; however, on the other hand, the entire communication network is too large to model and optimize using MoM or finite-element method techniques alone. The solution is to use both full-wave and TL models in a hybrid approach, which is formulated in the following sections with examples to demonstrate the efficiency, accuracy, and modeling versatility it can offer.

2. Formulating the Hybrid Approach

When constructing the hybrid models, it is important to both maintain accuracy and minimize solution times. That is, when properly implemented, a hybrid model should yield results consistent with its full-wave counterpart (i.e., no TL equations) and reduce the corresponding calculation time. MF propagation in a coal mine, whether along multiple conductors in a DM state or those involving lossy earth return paths, can commonly be approximated as transverse electromagnetic (TEM) modes [40]. When a quasi-TEM approximation is valid, full-wave sections in an MoM model can be represented by TL equations; this is how the hybrid approach is constructed. Full-wave sections are

strategically retained within a hybrid model to include local effects such as antenna-line coupling and other near-field interactions that are difficult to generalize with TL equations. This general idea is illustrated in Figure 1.

2.1 Formulation Methods

There are two major steps to perform when constructing a hybrid model for a given MF communication system: 1) determine adequate sizes for all full-wave sections, capable of capturing sufficient detail of the near-field interactions within the system, and 2) determine the TL equations that best represent the uniform MF propagation occurring in the coal mine communication network. In other words, “what is the correct ratio of full-wave sections to TL equation sections?” This is important since the smaller and less frequent the full-wave sections are, the smaller the resulting computational cost will be.

Starting with the determination of the full-wave sections, consider two examples of particular interest for analyzing and optimizing the survivability of a communication network. First, consider a TL excited by a transmitting antenna. The length of the full-wave section in the vicinity of the transmitter must be adequately long in order to capture the correct antenna-to-line coupling. A hybrid model with this type of full-wave section could be used to determine how best to excite an MF communication network in an underground mine. That is, because the antenna coupling section is modeled using full-wave techniques, it would be straightforward to move the antenna, change its orientation, or change its position and then use the TL equations within the hybrid approach to calculate the impressed currents on the remainder of the communication network. For the second important example, consider a broken TL due to a collapsed tunnel. Again, it is extremely important to use a full-wave region sufficiently large enough to accurately model the power losses associated with the broken TL.

Based on the experience gained from this work, there is no generalizable procedure that can answer how much of a given MF communication network should be modeled using full-wave sections and how much can be modeled using TL equations. In fact, this highlights the motivation behind the hybrid approach. That is to say, if the designer could trivially model and predict how various antennas would couple to a given communication network and how that network would respond to extreme environmental changes induced by a mine collapse, then analytical expressions, such as TL equations, would suffice alone. Unfortunately, this modeling task is not so straightforward. Hence, choosing the appropriate full-wave sections must be done on a case-by-case basis.

To show how this was typically done in this work, an example was constructed, which is outlined in Figure 2a, showing a twin-lead TL having a separation distance of 2 m and a wire radius of 1 mm ($Z_0 = 911\Omega$). The TL, which was terminated at both ends with loads Z , was positioned near two small loop antennas (20-cm diameter) separated by a distance L that were displaced from the plane of the TL by a distance x . The objective in this example was to determine what length of the TL near the two antennas must be modeled using MoM in order to accurately calculate the power transferred from T_x , operating at 500 kHz, to R_x . First, for a given L and x , the power transfer was calculated using strictly moment method (i.e., no TL equations) to establish a baseline. Then, a hybrid model was created starting

with full-wave sections 2 m long, symmetrically positioned about the antennas' respective positions. Next, the power transfer for shorted, matched, and open terminations was calculated. If the power transfers were within 10% accuracy of their full-wave-only counterparts, then the goal was met. If the power transfer error for any termination type was greater than 10%, the full-wave section of the hybrid model was increased by 2 m, and the power transfers were calculated again. This process was subsequently continued until the accuracy goal was met and was performed for three different L values (0.7, 1, and 2 km), each with 11 different x values (linearly spaced from 0 to 50 m). The result from this experiment is shown in Figure 2b, where it is clear that as the antenna was positioned further from the TL, the length of the full-wave section must be increased for a fixed accuracy criterion. In all cases investigated, the required full-wave section length was subwavelength ($\lambda_0 \approx 600$ m). It is also apparent that this relationship was independent of L due to the identical TL characteristics in each case.

Note that although this example suggested rather short full-wave sections were required to model accurate antenna coupling, all of the examples explored in the remainder of this paper made use of longer ($\sim \lambda/4$ to $\lambda/2$) full-wave sections. The main reason for this was so that when presenting hybrid model calculations, the variations in line current magnitude and phase could be easily identified and compared with the full-wave equivalent models.

In order to apply TL equations to the hybrid models, the propagation constant and characteristic impedance associated with the system must be calculated beforehand. With these data, TL equations may be formulated to calculate the equivalent loading and excitation on the full-wave sections associated with the sources and loads (e.g., transmitters and receivers), respectively. The TL propagation constant and characteristic impedance can be calculated using either numerical or analytical techniques. Typically, closed-form solutions are preferred due to the ease with which calculations can be made; however, they are not always available for the diverse range of geometries and materials commonly encountered in coal mines. Many times, only approximate solutions or more complex modal equations can be formulated. In this respect, it can be most straightforward to use available commercial codes to model prescribed geometries and calculate the associated propagation characteristics. For example, when considering low-loss TL, it can be shown that the propagation phase and attenuation constants are approximated by [36]

$$\beta = \frac{1}{2L} \left(\arctan \left[\frac{\text{Im} \left(\frac{1+A}{1-A} \right)}{\text{Re} \left(\frac{1+A}{1-A} \right)} \right] + 2m\pi \right) \quad (1)$$

$$\alpha = \frac{1}{2L} \ln \left| \frac{1+A}{1-A} \right|. \quad (2)$$

Here, L is the length of the TL, m is a nonnegative integer, and $A = \sqrt{Z_{sc}/Z_{oc}}$, where Z_{sc} and Z_{oc} are the input impedances for shorted and open terminations, respectively. Finally, the characteristic impedance can be calculated by [47]

$$Z_0 = \sqrt{Z_{oc} Z_{sc}}. \quad (3)$$

This way, the parameters required for the TL equations of the hybrid approach can be solved by calculating only the input impedances corresponding to open and shorted terminations. This technique, when applied to modeling performed with commercial codes, provides an efficient alternative when straightforward analytic methods are not available. Once propagation characteristics have been calculated, TL equations can be implemented in the hybrid approach and subsequently applied to optimization procedures. The remainder of this paper will concentrate on examples where the hybrid approach was applied.

2.2 Initial Examples

Ultimately, it is desired to model and optimize full-scale mines with the hybrid approach. Before this is done, it is instructive to demonstrate the efficiency and accuracy of the hybrid approach for a less complex geometry. The initial example considered demonstrates the accurate modeling of a TL T-intersection in free space, where Figure 3a details the geometry that was used. A 1-W ideal power source, operating at 500 kHz (free-space wavelength, $\lambda_0 \approx 600$ m) was used to feed the network. The twin-lead TLs were assigned a separation distance of 2 m and a wire radius of 1 mm. Each branch of the T-intersection was chosen to be 500 m long and was terminated with a load Z , which, for TL analysis, was chosen to be open, shorted, and matched. As shown in Figure 3a, three different hybrid models, i.e., Hybrids 1, 2, and 3, were considered and corresponded to utilizing ideal TL sections that were 100, 300, and 400 m long, respectively. The three hybrid models and the original full-wave model were compared in order to demonstrate the accuracy and increasingly reduced computational demands of the hybrid approach when larger and larger ideal TL sections were utilized, which effectively reduced the size of matrices used in MoM calculations. Figure 3b compares the calculated current profiles of the full-wave and hybrid models along the X- and Y-axis-aligned branches. The current calculations, which were normalized to the source current, indicate that the hybrid approach agreed well with its full-wave counterpart. Note that where current values have been omitted indicates the location of the analytic ideal TL sections. Finally, using an 8-core Intel E5620, hybrid models 1, 2, and 3 reduced simulation times by approximately 4, 20, and 80 times, respectively, compared with the equivalent full-wave model.

In the previous example, the computational time required by the hybrid model depended only on the size of full-wave sections used for the source and load regions. Subsequently, the hybrid approach allows networks to increase in size without discernible change in computational times, whereas an equivalent full-wave model using MoM would require more computational time and resources as the physical size of the model increases. This not only makes the hybrid approach attractive for large problems but also facilitates modeling of full-scale mines, whereas using MoM would not be feasible, even with notable computer resources.

In the next example, this fact was exploited and tested. Specifically, a TL $27 \lambda_0$ long at 500 kHz (i.e., 16.2 km) was placed between two parallel plates of lossy earth in order to test the hybrid model subject to environmental loading, which is an important consideration when

modeling MF communication networks in coal mines. The TL possessed the same separation and wire radius as in the previous example. A 10-cm radius loop antenna with a wire radius of 1 mm was used for both the transmitting (T_x) and receiving (R_x) antennas. T_x was fed by a 1-W power source operating at 500 kHz. This geometry is illustrated in Figure 4a. For this example, the environmentally-loaded TL equations were constructed using moment method models in conjunction with the techniques discussed in [36]. Currents along the full-wave section surrounding R_x were calculated for shorted and open terminations and are compared for the hybrid and full-wave models in Figure 4b. This example clearly demonstrates the accuracy of the hybrid approach, even over very large distances of propagation. Because of this large distance, computational times for the full-wave and hybrid models were 5540 and 6.9 s, respectively, on an 8-core Intel E5630. This equated to a factor of 800 reduction in computation time.

3. Propagation With an Earth Return

3.1 TL Approximations

In order to account for the various possible MF propagation modes in coal mines, it is also important to consider those that use the surrounding earth material as a current path. This may occur when either a multiple wire system is experiencing CM propagation or a single wire conductor is placed within the coal mine tunnel. In the following sections, the modeling of a single wire conductor placed close (i.e., much less than one wavelength) to a lossy earth material is considered. This geometry, as shown in Figure 5, can equivalently represent multiple wire conductors facilitating in-phase propagation (CM propagation) and subsequently using the earth as the current return path. As predicted in the literature [46], [48, 49], at MF, a quasi-TEM mode is readily established between a single conductor and earth material return path. Because of this characteristic, the modeling of a conductor positioned near a single earth layer should be a good approximation to an identical conductor placed nearest to one (out of four) of the boundaries within a mine tunnel (more on this and its importance shortly). This is a reasonable application since, in practice, conductors would usually be supported by ceilings or floors. As will be shown, with this approximation, the TL analysis is significantly simplified. However, it is worth noting that this approximation may not hold as well when the conductor is placed in a corner of the tunnel cross section, effectively placing it close to two intersecting earth surfaces. Developing accurate and efficient models for this scenario is a topic of future consideration.

Propagation with earth return has been a topic of interest for almost a century. First reported in 1926, Carson [49] derived approximate TL solutions under the assumption that the wires are thin, placed in close proximity to the ground, and that the ground return dissipation factor is characteristic of good conductors (i.e., $\sigma/\epsilon\omega \gg 1$). In effect, Carson's approximation provides straightforward calculations but requires low frequencies of operation and/or the return path to have high conductivity, which may not be the case for all mine materials of interest. Significant improvement was made in 1972, when the analysis of J. R. Wait [46] provided the exact modal equation for all ranges of both electrical and geometric parameters. Wait's model showed that the propagation constant, i.e., $j\gamma$, could be written in terms of the standard TL modal equation given by

$$j\gamma = \sqrt{ZY}, \quad (4)$$

where Z and Y are the equivalent series impedance and shunt admittance, respectively, and are functions of γ .

The difficulty with Wait's approach is that γ is a function of itself and therefore requires advanced numerical methods to compute solutions in all but the simplest cases. To avoid the challenges associated with solving the exact modal equation and obtain intuition for the system, attempts to improve on Carson's original approximation have been reported, which introduce corrective terms that account for displacement currents associated with lossy dielectrics. The approximation used here was reported in 1996 by D'Amore and Sarto [48], which is formulated in the Appendix. When compared with Wait's exact modal (4), this approximation is remarkably simple to use, so long as the appropriate limiting conditions are met, providing an accurate means to perform rapid computations of the propagation constant and characteristic impedance.

3.2 Hybrid Approach for a Wire With Earth Return

Next, a hybrid model was constructed using the D'Amore approximation outlined in the Appendix. The example considered was a wire placed 20 cm above an earth/air interface. The lossy earth return was assigned material parameters of $\sigma = 0.01$ S/m and $\varepsilon = 10$. The 5-km-long copper wire had a 1-mm radius and was terminated into the ground, normal to the air/earth surface boundary. The grounding rod was 1.5 m long and had a radius of 1 mm. At one end of the TL, there was an ideal voltage source operating at 500 kHz. At the opposite end, there was a load Z . The corresponding geometry is illustrated in Figure 6a. In this hybrid model, a 4.4-km-long section between the source and the load was replaced by TL equations constructed using the D'Amore approximation. Effectively, these TL equations were used to properly load the source section and excite the load section. Line currents were calculated and are compared in Figure 6b for the load Z designated to be both open and short. It is extremely important to note that there was an additional resistance associated with the grounding rod geometry (i.e., length and diameter) beneath the earth's surface, which can be seen from the reduced SWR of the so-called shorted currents. To account for this in the hybrid model, the resistance was approximated using the low-frequency power system equations for grounding rod resistance discussed in [50], which is given by

$$R_{term} = \frac{1}{2\pi\sigma l} \log\left(\frac{2l}{a}\right) \quad (5)$$

where σ is the ground conductivity, l is the length of the grounding rod, and a is the radius of the grounding rod. It is important to note that this equation assumes that the earth material surrounding the grounding rod is characteristic of a good conductor. This is often the case for MF propagation in coal mines; however, an alternative approach would be required for low-conductivity earth materials.

The current calculations in Figure 6b indicate only a small current error between the hybrid and full-wave models—approximately an error of 2 dB and 15 degrees in phase. Again, note

that the omission of currents in the hybrid model indicates where TL equations have been applied. The good agreement of current calculations for both termination types further indicates the accuracy of the D'Amore approximation for these geometries when excited with MF. Furthermore, using an 8-core Intel E5620, the hybrid models were simulated in 7.4 s. The full-wave counterpart was completed in 440 s, which corresponded to a factor of 60 reduction in computation time.

As was previously suggested, the D'Amore approximation can be effectively utilized due to the TEM nature of MF waves in coal mines, where most of the EM energy is confined between the wire conductor(s) and the nearest tunnel boundaries. The next example considered employing the hybrid technique to support this argument. In this example, we made use of the fact that if a wire conductor is positioned closer to one tunnel boundary than the others, such as is shown in Figure 7b, then the EM environment should be approximately equivalent to that shown in Figure 7a, which is the geometry that was just previously considered for a hybrid model.

In the next example, a 1-km-long wire conductor was positioned 50 cm above a mine tunnel floor. The tunnel cross section was assigned typical coal mine dimensions with a height of 2 m and a width of 6 m; however, due to the approximation used here, these dimensions were not expected to greatly affect the propagation characteristics. That is, only the mine floor material parameters and distance the wire was positioned from that surface would dictate the EM properties of the TL. An ideal voltage source operating at 500 kHz was positioned opposite to either a short or open termination. This geometry is illustrated in Figure 7c. Currents for the hybrid and full-wave models were calculated for both termination types and two different mine floor conductivities ($\epsilon_g = 10$): $\sigma_g = 1e-2$ S/m and $1e-3$ S/m. The corresponding currents that were calculated are compared in Figure 8. There was some disagreement in the calculated currents, likely due to additional loading from the other tunnel boundaries; however, overall, the results demonstrate the accuracy of the hybrid approach for mine tunnels where a single conductor is placed close to one of the boundaries. Again, it is important to note that this assumption will need further consideration and revision in geometries where the wire conductor is placed equally close to two intersecting surfaces. Furthermore, to add complexity to the system, the coal seam (i.e., tunnel walls) and conductive rock layers (i.e., ceiling and floor) generally have conductivities that differ by one to several orders of magnitude [27]. This is a topic to be considered in future work, but remember it is always possible to construct accurate TL models by applying the techniques formulated in [36] to representative full-wave models. To conclude this example with calculation time comparisons, the full-wave and hybrid models were simulated in 3800 and 720 s, respectively, on a 12-core Intel E5645. This equated to a factor of 5.2 reduction in the computation time. It is very important to note that for this example, the memory requirements were 37.7 and 4.6 GB for the full-wave and hybrid models, respectively. Hence, for typical computers, the coal mine tunnel length is very limited using full-wave techniques alone; only the hybrid approach can allow for substantial line lengths required to model large-scale coal mine communication networks. Furthermore, optimizing such networks without the hybrid method would be infeasible all together.

4. Large-scale Optimizations Using the Hybrid Approach

As previously mentioned, the main motivation behind the hybrid approach was to facilitate large-scale optimizations of coal mine communication networks that would otherwise be very challenging due to the limited analytic solutions or the large computational cost of full-wave (MoM) computer models. With the previous examples establishing the basic tools for constructing communication networks with the hybrid approach, two final optimization examples were formulated and are presented next.

The first example optimized power transfer from a single transmitter to three receivers through a large TL network placed in free space, as shown in Figure 9. Each segment of the TL network was 240 m long. Each antenna had a 10-cm diameter and a 1-W power source operating at 500 kHz. A binary genetic algorithm was used to maximize power transfer by choosing whether an open or short (i.e., one or zero bit) should be placed at each node and end termination. The goal of power maximization was achieved by implementing the following cost function:

$$\text{cost} = \sum_i |10 \log_{10}(P_i)| \quad (6)$$

where i represents each receiving antenna, and absolute values were imposed because evolutionary algorithms traditionally try to minimize cost. Each iteration of the optimization using the hybrid model required only 7.9 s on an 8-core Intel E5620. In comparison, the full-wave counterpart required 356 s, a runtime factor difference of about 45. To fully appreciate this time difference, consider that this example was converged by generation 25 using a population of 20. Hence, totaling 500 iterations for convergence, the hybrid approach required about 1 h, whereas optimizations employing the full-wave models would require approximately two days. The optimal solution is shown pictorially in Figure 9, where unfilled and filled circles represent open and shorted terminations, respectively. The hybrid model calculated power transfer from T_x to be -156.3 , -148.9 , and -157.4 dB to R_{x1} , R_{x2} , and R_{x3} , respectively. Using the same terminations in an equivalent full-wave model, the calculated power transfer was determined to be -156.3 , -148.6 , and -157.4 dB to R_{x1} , R_{x2} , and R_{x3} , respectively. Hence, even for a large communication network, the hybrid model produces extremely accurate results.

The second and final example optimized a communication network similar to what could be used within a room-and-pillar mine architecture such as that shown in Figure 10. To simplify the problem, conductors were placed much closer to the floor than to other surfaces, such as the coal pillars and ceiling, allowing the system to be approximated as if only the floor were present. The communication network used for optimization is shown in Figure 11a, which illustrates the top view of a series of single conductor interconnects that use the earth as a return path. The lossy earth layer was assigned material properties $\sigma = 0.01$ S/m and $\epsilon = 10$. All copper wires were positioned 20 cm offset from the air/earth interface. In this example, SWR was minimized by using the covariance matrix adaptation evolutionary strategy (CMA-ES) [51]. CMA-ES is a powerful evolutionary algorithm recently introduced to the EMs community [52], which moves a multivariate normally distributed population around the solution space. This algorithm has advantages over other

popular real-valued global optimization algorithms, such as particle swarm optimization, in that it maintains and exploits search history, allowing for small population sizes and, subsequently, accelerated and robust solution discovery. CMA-ES also has the advantage of requiring few user inputs, where only the independent input variable ranges and standard deviations are required from the user. For this hybrid optimization example, SWR was minimized by utilizing the cost function, i.e.,

$$\text{cost} = \sum_i \frac{\max |I_j|}{\min |I_j|} \quad (7)$$

where I_j are the currents on the wire sections closest to the transmitting and receiving antennas, which are represented by orange-dashed lines in Figure 11a. This was accomplished by simply extracting the calculated currents along the full-wave sections from the simulation output files. Subsequently, the corresponding SWR values were calculated and used as a feedback mechanism for CMA-ES. Network tuning was accomplished by varying the distance that the grounding rods penetrated into the ground (i.e., grounding rod length) at the end of each TL section, which effectively varied their individual termination resistances. The geometries of the transmitting antenna and two receiver antennas were identical: 10-cm loop antennas with 1-mm-radius wire. To excite the network, T_x was fed by a 1-W ideal power source operating at 500 kHz. Only the 200-m full-wave sections nearest to the antennas were left in the hybrid model. Figure 11b compares the currents calculated in the optimized hybrid model and the equivalent full-wave model. All currents were normalized to the source current on T_x in order to indicate overall power transfer from T_x to R_{x1} and R_{x2} . The agreement between currents was extremely good considering the beneficial improvement in computational speed. The full-wave models required 1157 s to simulate on an 8-core Intel E5620. On the same machine, the hybrid model required only 10.7 s, providing a runtime reduction factor of 110.

Finally, to further demonstrate the power of the hybrid approach, a TL break (1-cm section removed), simulating a mine collapse, was introduced into the communication network, represented by a red “X” in Figure 11a. Such an EM model would not be easily represented using simple TL equations. However, using the hybrid method, a full-wave section introduced to model the line break fully captured the propagation effects and associated power losses. The currents predicted by the hybrid model were calculated and are compared with the equivalent full-wave model in Figure 11b. The reliability and versatility of the hybrid approach for near-field effects such as line breaks will be crucial for performing parametric studies on communications systems designed for emergency response in coal mines and improved survivability.

5. Conclusion

The hybrid approach was shown to significantly improve computational efficiency while simultaneously providing a high degree of precision. First, TLs making a T-intersection placed in free space were verified. Then, geometries that utilize earth materials as a current return path were approximated using D’Amore’s method. From this approximation,

appropriate TL equations were implemented into both above earth and coal mine tunnel hybrid models, which were validated through comparisons with full-wave simulations. With these basic tools, it was demonstrated that full-scale coal mine communication networks can be constructed and optimized both for daily operations as well as emergency communications and tracking. Future work will include comparing the outlined design techniques and optimized coal mine communication networks with measurements to further verify the accuracy of the hybrid method. It will also be important to extend the hybrid approach to accommodate multimodal/multiconductor TLs. The combined methods of numerical and analytic modeling with measurements should provide a powerful engineering package for future system design.

Acknowledgments

The findings and conclusions in this paper are those of the authors and do not necessarily represent the views of the National Institute for Occupational Safety and Health (NIOSH). Mention of any company name or product does not constitute endorsement by NIOSH.

This work was supported in part by the Centers for Disease Control and Prevention contract number 200-2010-36317.

References

1. Murphy JN, Parkinson HE. Underground Mine Communications. Proceedings of the IEEE. Jan; 1978 66(1):26–50.
2. Bandyopadhyay, LK.; Chaulya, SK.; Mishra, PK. Wireless Communication in Underground Mines: RFID-based Sensor Networking. New York: Springer; 2009.
3. Schiffbauer WH, Brune JF. Coal Mine Communications. American Longwall Magazine. 2006:24–25.
4. Forooshani AE, Bashir S, Michelson DG, Noghianian S. A Survey of Wireless Communications and Propagation Modeling in Underground Mines. IEEE Communications Surveys and Tutorials. 2013; 15(4):1524–1545. Fourth Quarter.
5. Yarkan S, Guzelgoz S, Arslan H, Murphy RR. Underground Mine Communications: A Survey. IEEE Communications Surveys and Tutorials. 2009; 11(3):135–142. Third Quarter.
6. Dudley DG, Lienard M, Mahmoud SF, Degauque P. Wireless Propagation in Tunnels. IEEE Antennas and Propagation Magazine. Apr; 2007 49(2):11–26.
7. Emslie AG, Lagace RL, Strong PF. Theory of the Propagation of UHF Radio Waves in Coal Mines Tunnels. IEEE Trans Antennas and Propagation. Mar; 1975 AP-23(2):192–205.
8. Delogne P. EM Propagation in Tunnels. IEEE Trans Antennas and Propagation. Mar; 1991 AP-39(3):401–406.
9. Zhang YP, Zheng GX, Sheng JH. Radio Propagation at 900 MHz in Underground Coal Mines. IEEE Trans Antennas and Propagation. May; 2001 AP-49(5):757–762.
10. Zhang YP. Novel Model for Propagation Loss Prediction in Tunnels. IEEE Trans Vehicular Technology. Sep; 2003 52(5):1308–1314.
11. Boutin M, Benzakour A, Despins CL, Affes S. Radio Wave Characterization and Modeling in Underground Mine Tunnels. IEEE Trans Antennas and Propagation. Feb; 2008 AP-56(2):540–549.
12. Mahmoud SF. Modal Propagation of High Frequency Electromagnetic Waves in Straight and Curved Tunnels Within the Earth. Journal of Electromagnetic Waves and Applicatons. 19(12): 1611–1627.
13. Sun Z, Akyildiz I. Channel Modeling and Analysis for Wireless Networks in Underground Mines and Road Tunnels. IEEE Trans Communications. Jun; 2010 58(6):1758–1768.

14. Holloway CL, Hill DA, Dalke RA, Hufford GA. Radio Wave Propagation Characteristics in Lossy Circular Waveguides Such as Tunnels, Mine Shafts and Boreholes. *IEEE Trans Antennas and Propagation*. Sep; 2000 AP-48(9):1354–1366.
15. Dudley DG, Mahmoud SF. Linear Source in a Circular Tunnel. *IEEE Trans Antennas and Propagation*. Jul; 2006 AP-54(7):2034–2047.
16. Hill, DA.; Wait, JR. US Bureau of Mines Contract No J0113058. May. 1982 Theoretical Noise and Propagation Models for Through-the-earth Communications.
17. Durkin, JA. US Bureau of Mines Report of Investigations 8869 NTIS PB84-213792. 1984. Apparent Earth Conductivity over Coal Mines as Estimated from Through-the-Earth Electromagnetic Transmission Tests.
18. Pittman, W.; Church, R.; McLendon, JT. Through-the-earth Electromagnetic Trapped Miner Location Systems: A Review. U.S. Bureau of Mines; 1985.
19. Barkand TD, Damiano NW, Shumaker WA. Through-the-earth, Two-Way, Mine Emergency, Voice Communication System. *IEEE Industry Applications Conference*. Oct.2006 :955–958.
20. Yan L, Waynert JA, Sunderman C. Measurements and Modeling of Through-the-earth Communications for Coal Mines. *IEEE Trans Industrial Applications*. Sep-Oct;2013 49(5):1979–1983.
21. Cory, TS. US Bureau of Mines Purchase Order No PO382223. Dec. 1978 Antenna Design and Coupling Studies at Medium Frequency for Improved Coal Mine Communications.
22. Sacks, HK.; Chufo, RL. Medium-Frequency Propagation in Coal Mines. 4th WVU Conference on Coal Mine Electrotechnology; Aug. 2–4, 1978; p. 27-1-27-12.
23. Chufo, RL. Medium Frequency Mine Communications. 28th IEEE Vehicular Technology Conference; Mar. 1978; p. 261-266.
24. Stolarczyk, LG. US Bureau of Mines Contract No H0308004. Sep. 1984 A Medium Frequency Wireless Communication System for Underground Mines.
25. Lagace, RL.; Curtis, DA.; Foulkes, JD.; Rothery, JL. US Bureau of Mines Contract No H0346045. May. 1977 Transmit Antennas for Portable VLF to MF Wireless Mine Communications.
26. Dobroski, HH.; Stolarczyk, LG. Whole-Mine Medium-Frequency Radio Communication System. 6th WVU Conference on Coal Mine Electrotechnology; Jul. 1982; p. 124-136.
27. Lagace, RL.; Emslie, AG.; Grossman, MA. A. D. Little Inc. US Bureau of Mines Contract No H0346045. Feb. 1980 Modeling and Data Analysis of 50 to 5000 kHz Radio Wave Propagation in Coal Mines.
28. Cory, TS. US Bureau of Mines Contract No H0366028. Aug. 1977 Propagation of EM Signal in Underground Mines.
29. Cory, TS. US Bureau of Mines Contract No H0377053. Jun. 1978 Electromagnetic Propagation in Low Coal Mines at Medium Frequencies.
30. Stolarczyk LG. Emergency and Operational Low and Medium Frequency Band Radio Communications System for Underground Mines. *IEEE Trans Industrial Applications*. Jul-Aug; 1991 27(4):780–790.
31. Emslie AG, Lagace RL. Propagation of Low and Medium Frequency Radio Waves in a Coal Seam. *Radio Science*. Apr; 1976 11(4):253–261.
32. Hill DA. Electromagnetic Wave Propagation in an Asymmetrical Coal Seam. *IEEE Trans Antennas and Propagation*. Feb; 1986 AP-34(2):244–247.
33. Novak T, Snyder DP, Kohler JL. Postaccident Mine Communications and Tracking Systems. *IEEE Trans Industrial Applications*. Mar-Apr;2010 46(2):712–719.
34. Brockner, DE.; Werner, PL.; Werner, DH.; Waynert, J.; Li, J.; Damiano, NW. Characterization of Medium Frequency Propagation on a Twin-Lead Transmission Line with Earth Return. *IEEE International Symposium on Antennas and Propagation*; Jul. 2012; p. 1-2.
35. Brockner DE, Waynert J, Li J, Damiano NW, Werner DH, Werner PL. Modeling of Medium Frequency Propagation Experiments at the NIOSH Safety Research Coal Mine. *ACES International Review of Progress in Applied Computational Electromagnetics*. Mar.2013 :1–6.

36. Li J, Waynert JA, Whisner BG. An Introduction to a Medium Frequency Propagation Characteristic Measurement Method of a Transmission Line in Under-ground Coal Mines. *Progress in Electromagnetics Research B*. Sep.2013 55:131–149.
37. Li, J.; Whisner, B.; Waynert, JA. Measurements of Medium Frequency Propagation Characteristics of a Transmission Line in an Underground Coal Mine. *IEEE Industry Applications Society Annual Meeting*; Oct. 2012; p. 1-8.
38. Brandao Faria JA. Approximate Evaluation of the Wave Propagation Parameters of MF TL Communication systems for Mine Tunnels Using Image Theory. *Journal of Electromagnetic Waves and Applications*. Jan; 2014 28(4):515–530.
39. Hill DA, Wait JR. Excitation of Monofilar and Bifilar Modes on a Transmission Line in a Circular Tunnel. *Journal of Applied Physics*. Aug; 1974 45(8):3402–3406.
40. Mahmoud SF. On the Attenuation of Monofilar and Bifilar Modes in Mine Tunnels. *IEEE Trans Microwave Theory and Techniques*. Sep; 1974 22(9):845–847.
41. Mahmoud SF, Wait JR. Calculated Channel Characteristics of a Braided Coaxial Cable in a Mine Tunnel. *IEEE Trans Communications*. Jan; 1976 24(1):82–87.
42. Paul, CR. *Analysis of Multiconductor Transmission Lines*. 2. New York: John Wiley; 2007.
43. D'Amore M, Sarto MS. Simulation Models of a Dissipative Transmission Line Above a Lossy Ground for a Wide-frequency Range—Part II: Multiconductor Configuration. *IEEE Trans Electromagnetic Compatibility*. May; 1996 38(2):139–149.
44. Dounavis A, Achar R, Nakhla M. A General Class of Passive Macromodels for Lossy Multiconductor Transmission Lines. *IEEE Trans Microwave Theory and Techniques*. Oct; 2001 49(10):1686–1696.
45. Mahmoud SF, Wait JR. Theory of Wave Propagation Along a Thin Wire Inside a Rectangular Waveguide. *Radio Science*. Mar; 1974 9(3):417–420.
46. Wait JR. Theory of Wave Propagation Along a Thin Wire Parallel to an Interface. *Radio Science*. Jun; 1972 7(6):675–679.
47. Pozar, DM. *Microwave Engineering*. 2. New York: John Wiley; 1998.
48. D'Amore M, Sarto MS. Simulation Models of a Dissipative Transmission Line Above a Lossy Ground for a Wide-frequency Range—Part I: Single Conductor Configuration. *IEEE Trans Electromagnetic Compatibility*. May; 1996 38(2):127–138.
49. Carson JR. Wave Propagation in Overhead Wires with a Ground Return. *Bell System Technical Journal*. Oct.1926 5:539–554.
50. King, RL.; Hill, HW., Jr; Bafanna, RR.; Cooley, WL. US Bureau of Mines, Information Circular 8767. 1978. Guide for the Construction of Driven-Rod Ground Belts.
51. Hansen N, Müller SD, Koumoutsakos P. Reducing the Time Complexity of the Derandomized Evolution Strategy with Covariance Matrix Adaptation (CMA-ES). *Evolutionary Computation*. Spring;2003 11(1):1–18. [PubMed: 12804094]
52. Gregory MD, Bayraktar Z, Werner DH. Fast Optimization of Electromagnetic Design Problems Using the Covariance Matrix Adaptation Evolutionary Strategy. *IEEE Trans Antennas and Propagation*. Apr; 2001 AP-59(4):1275–1285.

Biographies



Donovan E. Brockner received the B.S. degree in electrical engineering from the University of Wisconsin—Milwaukee, Milwaukee, WI, USA, in 2010. He is currently working toward

the Ph.D. degree in electrical engineering at the Pennsylvania State University, University Park, PA, USA.

He is a Research Assistant with the Computational Electromagnetics and Antennas Research Lab. His research interests include computational electromagnetics, metamaterials, geoelectromagnetics, and nanoelectromagnetics.



Peter E. Sieber received the B.S. degree in electrical engineering (with honors) from the University of Wisconsin—Milwaukee, Milwaukee, WI, USA, in 2009. He is currently working toward the Ph.D. degree at the Pennsylvania State University, University Park, PA, USA.

He is a Graduate Research Assistant for Dr. Werner with the Computational Electromagnetics and Antennas Research Lab. His research interests include nanotechnology, antenna engineering, metamaterials, and computational electromagnetics.

Mr. Sieber is a member of the Tau Beta Pi and Phi Kappa Phi honor societies and has served as the UWM-IEEE student chapter president.



Joseph A. Waynert (°1986) received the Ph. D. degree in physics from the University of Wisconsin—Milwaukee, Milwaukee, WI, USA.

He is an Acting Team Leader with the National Institute for Occupational Safety and Health (NIOSH). Prior to NIOSH, he worked in the industry investigating methods of improved spectrum management for the military. Previous to that, he was with the Los Alamos National Lab, developing applications of applied superconductors. His primary research focuses on wireless communications and electronic tracking. In particular, he is experimentally and theoretically investigating the mechanisms controlling path loss in underground coal mining applications. System frequency bands of interest include extremely low frequency, medium frequency, and ultrahigh frequency.



Jingcheng Li received the B.S. degree in electrical engineering from China University of Mining and Technology, Beijing, China, in 1982 and the M.S. and Ph.D. degrees in mining engineering, specializing in electrical engineering applications in mining engineering, from the Pennsylvania State University, University Park, PA, USA, in 1992 and 1996, respectively.

He is a Senior Service Fellow with the National Institute for Occupational Safety and Health. Previously, he was a Senior Software Engineer with Analog Devices, Inc. (ADI). Prior to ADI, he was an Instructor with the Department of Electrical and Automation Engineering, China University of Mining and Technology. His primary research interests are in underground communications and tracking and proximity detection. In particular, he is currently focused on investigating medium-frequency propagation characteristics in underground mines, modeling of magnetic field distribution, and precise locating architecture of magnetic proximity detection systems.

Dr. Li received the First Prize Paper Award and the Prize Paper Award in 1995 and 2000, both shared with Dr. J. Kohler, from the IEEE.



Pingjuan L. Werner received her Ph.D from the Pennsylvania State University in 1991.

She is a Professor with the Pennsylvania State University College of Engineering, University Park, PA, USA. Her primary research focuses are in the area of electromagnetics, including fractal antenna engineering and the application of genetic algorithms in electromagnetics.

Ms. Werner received the Best Paper Award from the Applied Computational Electromagnetics Society in 1993. She is a member of the Tau Beta Pi National Engineering Honor Society, the Eta Kappa Nu National Electrical Engineering Honor Society, and the Sigma Xi National Research Honor Society.



Douglas H. Werner received the B.S., M.S., and Ph.D. degrees in electrical engineering and the M.A. degree in mathematics from the Pennsylvania State University (Penn State), University Park, PA, USA, in 1983, 1985, 1989, and 1986, respectively.

He holds the John L. and Genevieve H. McCain Chair Professorship in the Pennsylvania State University Department of Electrical Engineering. He is the Director of the Computational Electromagnetics and Antennas Research Lab (<http://cearl.ee.psu.edu/>) and a member of the Communications and Space Sciences Lab. He is also a faculty member of the Materials Research Institute, Penn State. He holds seven patents, has published over 600 technical papers and proceedings articles, and is the author of 12 book chapters with two additional chapters currently in preparation. He has published several books, including *Frontiers in Electromagnetics* (Piscataway, NJ: IEEE Press, 2000), *Genetic Algorithms in Electromagnetics* (Hoboken, NJ: Wiley/IEEE, 2007), and *Transformation Electromagnetics and Metamaterials: Fundamental Principles and Applications* (London, U.K.: Springer, 2014). He has also contributed chapters for several books, including *Electromagnetic Optimization by Genetic Algorithms* (New York: Wiley Interscience, 1999), *Soft Computing in Communications* (New York: Springer, 2004), *Antenna Engineering Handbook* (New York: McGraw-Hill, 2007), *Frontiers in Antennas: Next Generation Design and Engineering* (New York: McGraw-Hill, 2011), *Numerical Methods for Metamaterial Design* (New York: Springer, 2013), and *Computational Electromagnetics* (New York: Springer, 2014). His research interests include computational electromagnetics, antenna theory and design, phased arrays (including ultrawideband arrays), microwave devices, wireless and personal communication systems (including on-body networks), wearable and e-textile antennas, radio-frequency identification tag antennas, conformal antennas, reconfigurable antennas, frequency-selective surfaces, electromagnetic wave interactions with complex media, metamaterials, electromagnetic bandgap materials, zero- and negative-index materials, transformation optics, nanoscale electromagnetics (including nanoantennas), fractal and knot electrodynamics, and nature-inspired optimization techniques (genetic algorithms, clonal selection algorithms, particle swarm optimization, wind-driven optimization, and various other evolutionary programming schemes).

Dr. Werner was presented with the 1993 Applied Computational Electromagnetics Society (ACES) Best Paper Award and was also a recipient of the 1993 International Union of Radio Science (URSI) Young Scientist Award. In 1994, he received the Pennsylvania State University Applied Research Laboratory Outstanding Publication Award. He was a coauthor (with one of his graduate students) of a paper published in the IEEE Transactions on Antennas and Propagation that received the 2006 R. W. P. King Award. In 2011, he received the inaugural IEEE Antennas and Propagation Society Edward E. Altshuler Prize

Paper Award. He has also received several Letters of Commendation from the Pennsylvania State University Department of Electrical Engineering for outstanding teaching and research. He is a former Associate Editor of *Radio Science*, an Editor of the IEEE Antennas and Propagation Magazine, and a member of the American Geophysical Union, URSI Commissions B and G, ACES, Eta Kappa Nu, Tau Beta Pi, and Sigma Xi. He was a recipient of a College of Engineering PSES Outstanding Research Award and Outstanding Teaching Award in March 2000 and March 2002, respectively. He was also presented with an IEEE Central Pennsylvania Section Millennium Medal. In March 2009, he received the PSES Premier Research Award. He is a Fellow of the Institute of Engineering and Technology (formerly IEE) and the ACES.

7. Appendix

The approximation used for single-wire configurations with an earth return, which has been implemented here in the hybrid approach, was reported in 1996 by D'Amore and Sarto [48]. The derivation assumes a thin-wire diameter, and wire heights are much smaller than one wavelength (i.e., $a \ll \lambda$ and $h \ll \lambda$ in Figure 5, respectively). With these assumptions, the approximate form of the propagation constant in (4) is given by

$$\gamma^2 \approx k_0^2 \left(\frac{\frac{2\pi Z_{\text{int}}}{j\omega\mu_0} + \ln\left(\frac{2h}{a}\right) + 2S_1(h)}{\ln\left(\frac{2h}{a}\right) + S_2(h)} \right) \quad (8)$$

where Z_{int} is the wire's internal impedance, whereas S_1 and S_2 are the small argument, logarithmic approximations for the associated Sommerfeld integrals given by

$$S_1(h) = \frac{1}{2} \ln(1 + \alpha r^{-1}) \quad (9)$$

$$S_2(h) = \frac{k_0^2}{k_g^2 + k_0^2} \ln(1 + \beta r^{-1}). \quad (10)$$

Here, jk_0 and jk_g are the propagation constants of unbounded EM waves in the free space and ground media, respectively. Finally, $r = (4h^2 + a^2)^{1/2}$, where h is the distance from the earth/free-space boundary to the center of a wire conductor with radius a , shown in Figure 5. The α and β terms are defined by

$$\alpha = \frac{2}{\sqrt{k_0^2 - k_g^2}} \quad (11)$$

$$\beta = \frac{k_0^2 + k_g^2}{k_0^2 \sqrt{k_0^2 - k_g^2}}. \quad (12)$$

Note that the propagation constant, i.e., γ , is no longer a function of itself, making subsequent TL equations in the hybrid approach a straightforward task.

Author Manuscript

Author Manuscript

Author Manuscript

Author Manuscript

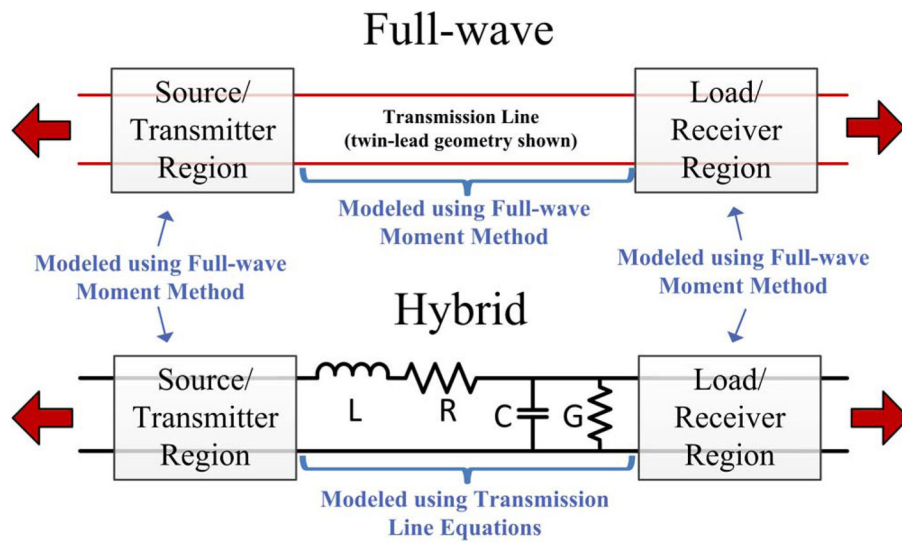
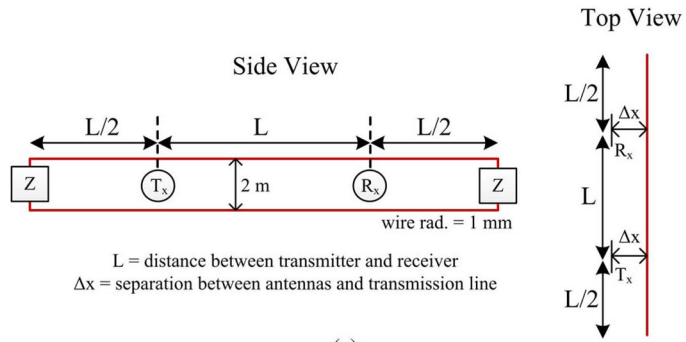
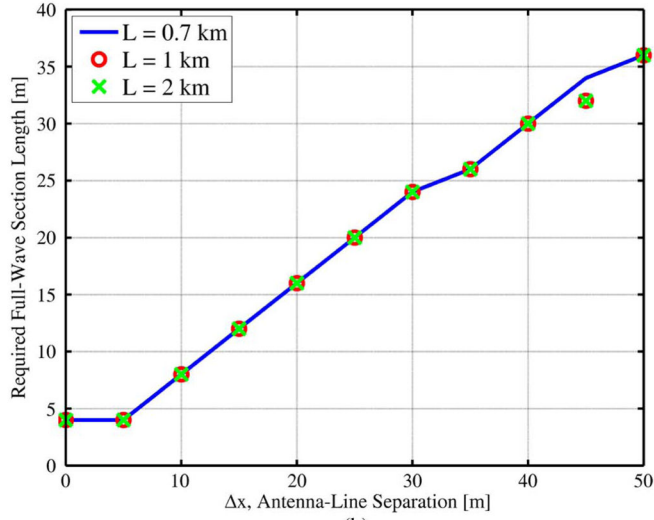


Figure 1. Comparison of a strictly full-wave model to a hybrid model using both full-wave regions and TL equations.



(a)



(b)

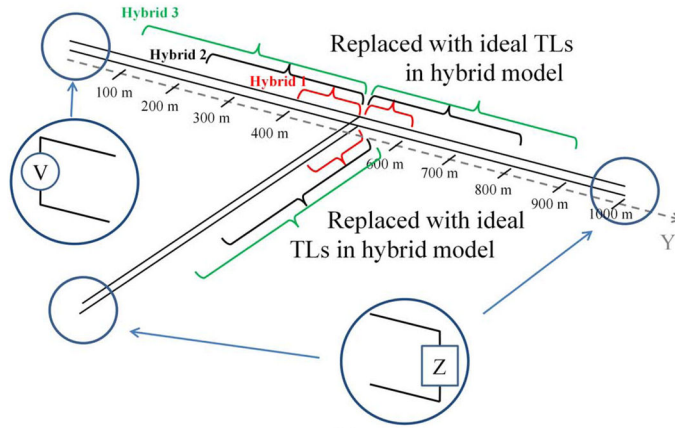
Figure 2. (a) Example geometry constructed to determine the full-wave sections required to accurately calculate power transfer from T_x to R_x . (b) Required length of full-wave (moment method) section to accurately couple EM energy from a small antenna element to the twin lead TL shown in (a).

Author Manuscript

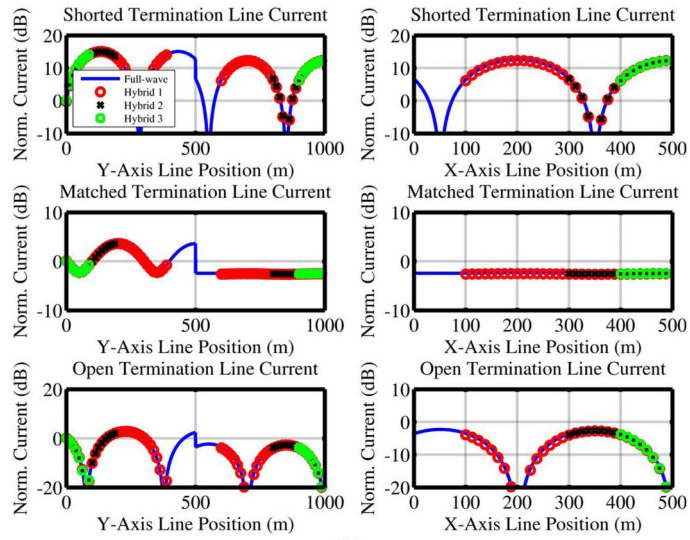
Author Manuscript

Author Manuscript

Author Manuscript



(a)



(b)

Figure 3. (a) Geometry of a T-intersection full-wave and hybrid model comparison using open, shorted, and matched terminations. (b) Currents calculated using equivalent full-wave and hybrid models. The calculated current magnitudes were normalized to the source current.

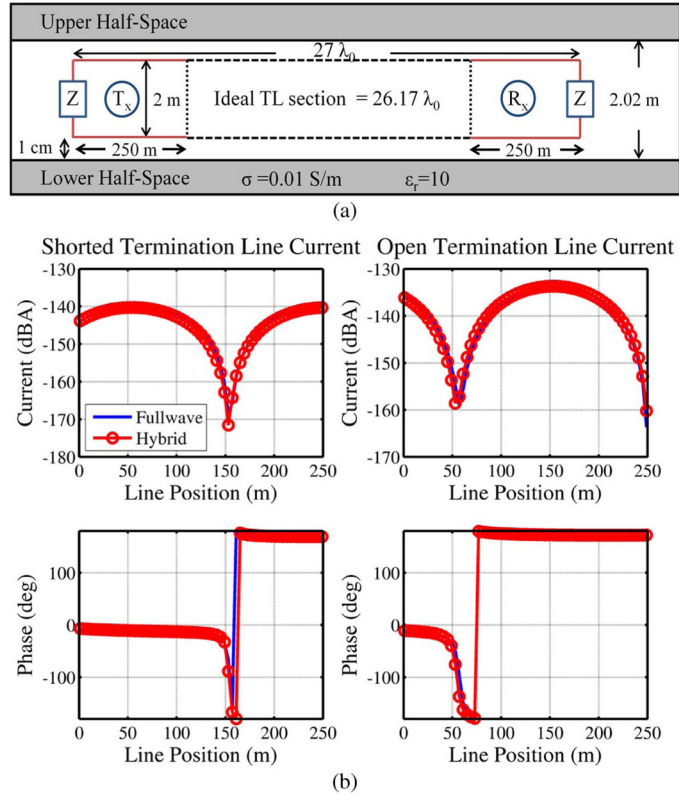


Figure 4. (a) Geometry of a $27 \lambda_0$ long TL (i.e., 16.2 km) placed between two parallel boundaries of lossy earth used to test the hybrid model subject to environmental loading. (b) Current magnitudes and phases calculated on the R_x TL section were compared between full-wave and hybrid models for shorted and open terminations.

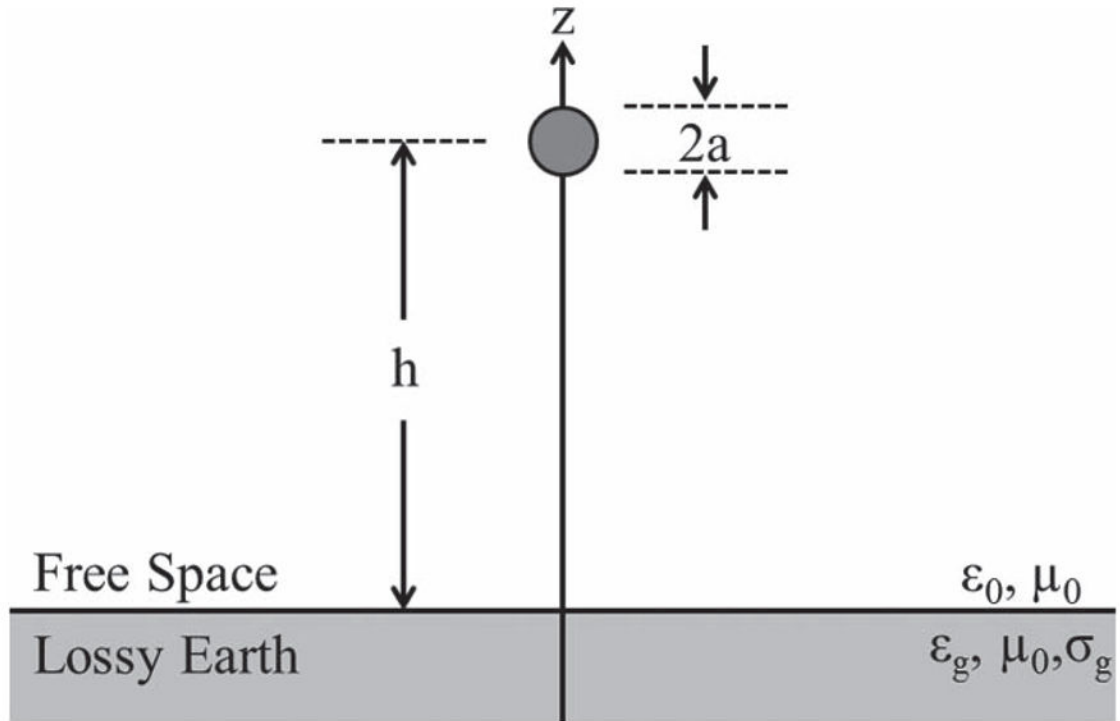


Figure 5.
Geometry of single wire above lossy earth and free-space boundary.

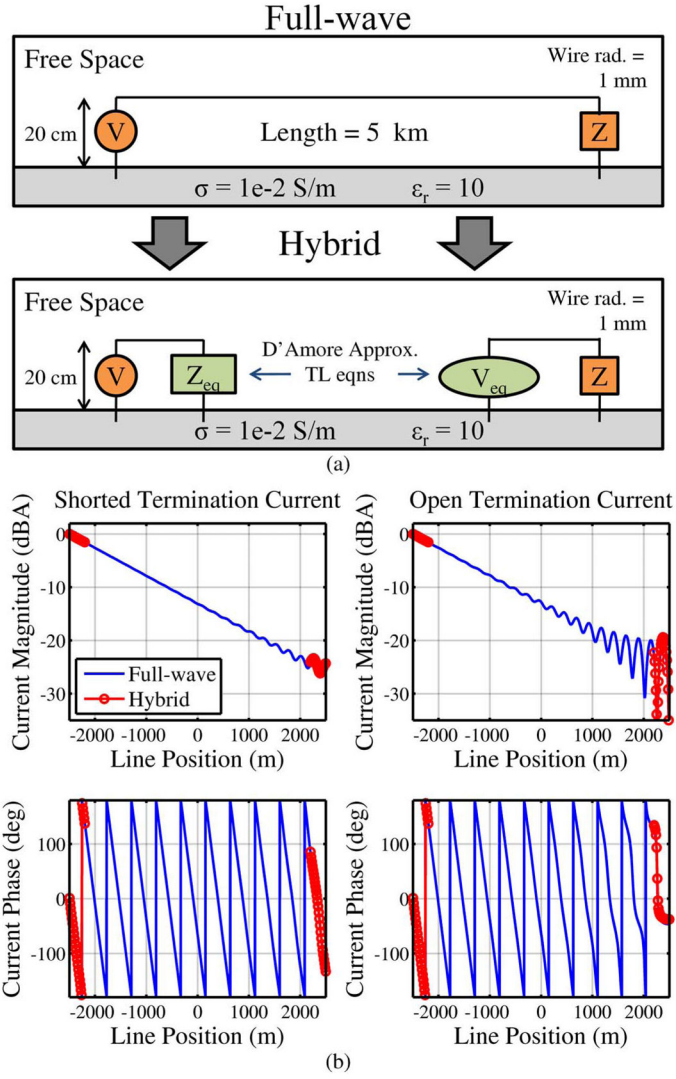


Figure 6. (a) Geometry: 1-mm-radius wire placed 20 cm above lossy earth return. (b) Currents for full-wave and hybrid models were calculated and are compared for both shorted and open terminations.

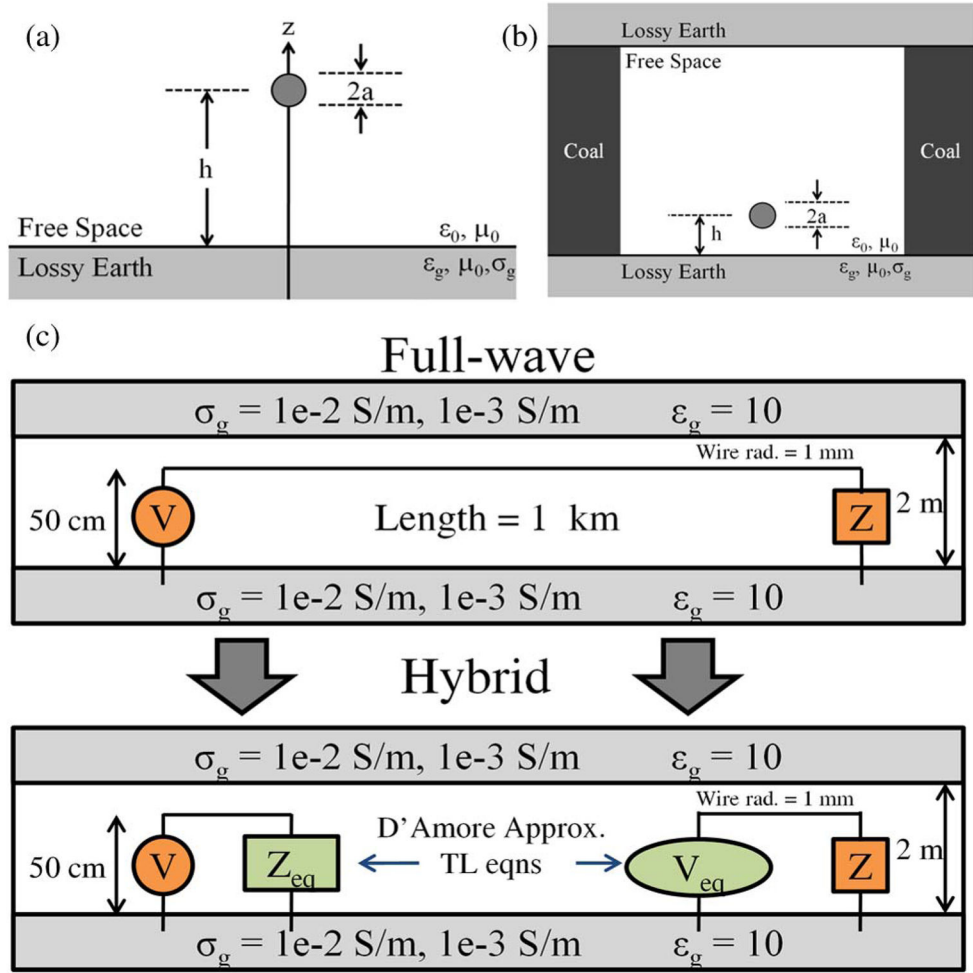


Figure 7. (a) Geometry: wire placed above a lossy earth return. (b) Geometry: wire placed above a mine tunnel floor. (c) Side view of a mine tunnel hybrid model with a wire positioned 50 cm above a mine floor.

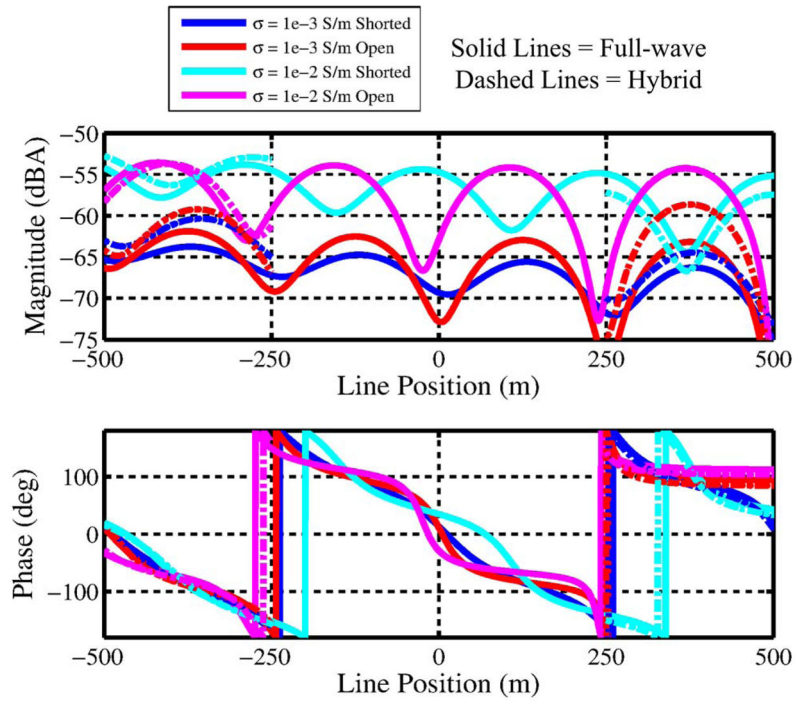


Figure 8. Currents for full-wave and hybrid models were calculated and are compared for both shorted and open terminations and two different return path conductivities.

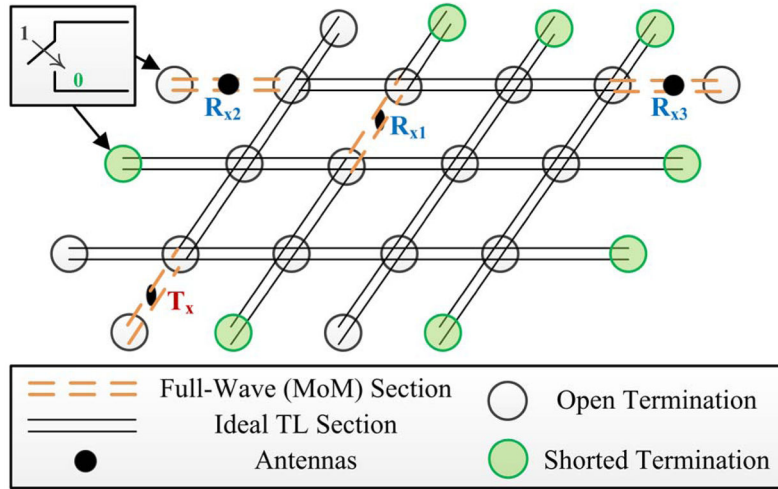


Figure 9. Large TL network used to demonstrate the feasibility of performing large-scale optimizations by utilizing the hybrid approach. The optimization protocol was to simultaneously maximize power transfer from T_x to three different receivers by implementing open and shorted terminations at each node and end load.

Author Manuscript

Author Manuscript

Author Manuscript

Author Manuscript



Figure 10.
Map of mining area showing room-and-pillar layout.

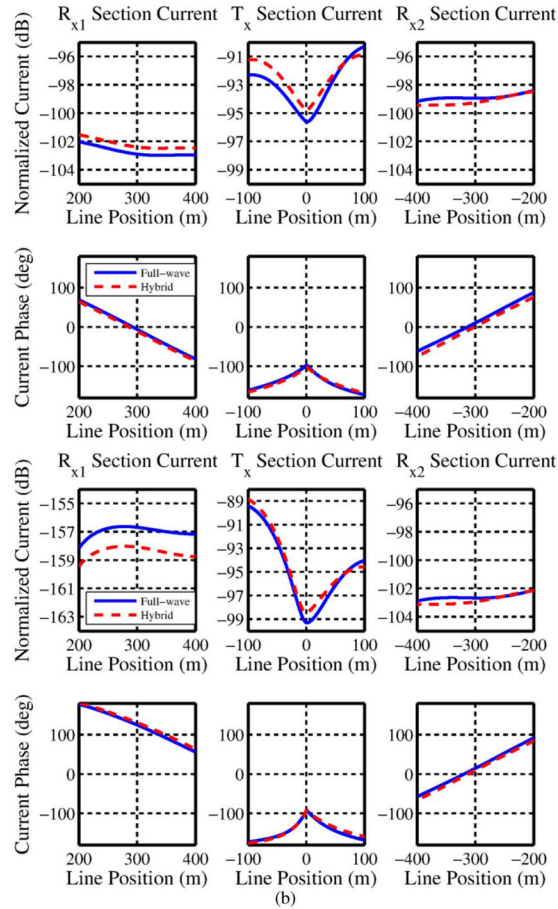
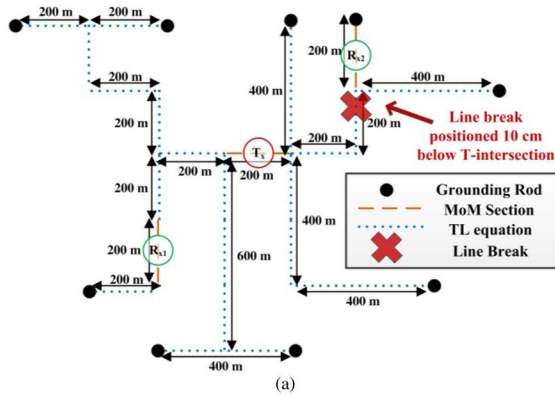


Figure 11.

(a) Geometry for optimization problem using the hybrid approach. A network of single conductors is constructed and optimized for minimum SWR on the segments nearest to the transmitter and receiving antennas. Optimization is performed by varying the length of grounding rods at the end of each open segment. (b) Top: Current comparison for optimized hybrid and full-wave models. Bottom: Current comparison for hybrid and full-wave models after a line break was introduced. The TL section corresponding to R_{x1} is located after the TL break, as is evident in the relatively small current magnitudes.